Type of the Paper (Article)

Supplementary Material: Coupled stratospheric chemistry-meteorology data assimilation. Part II: Weak and strong coupling

Richard Ménard[1*], Pierre Gauthier[4], Yves Rochon[1], Alain Robichaud[1], Jean de Grandpré[1], Yan Yang[1], Cécilien Charrette[3], and Simon Chabrillat[2].

[1] Air Quality Research Division, Environment and Climate Change Canada
[2] Belgium Institute for Space Aeronomy, Brussels, Belgium
[3] Meteorological Research Division, Environment and Climate Change Canada
[4] Département des sciences de la Terre et de l'atmosphère. Université du Québec à Montréal, Canada
* Correspondence: richard.menard@canada.ca; Tel.: +1-514-421-4613,
2121 Transcanada Highway, Dorval, (QC), CANADA, H9P 1J3

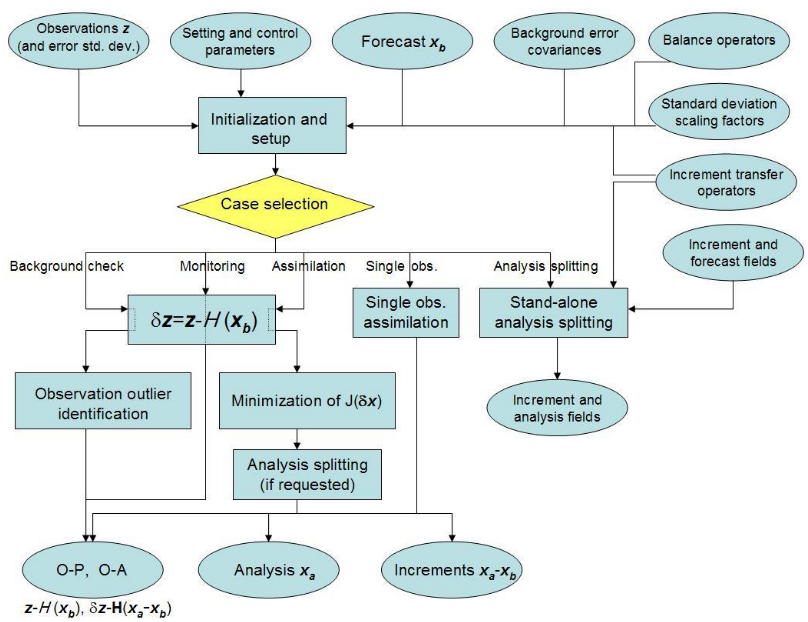

Figure S1. Flow chart covering the main steps and options of the 3D-Var-Chem.

Figure S1 provides a summary of some of the main steps and options of the 3D-Var-Chem, omitting here some of the various intermediate steps. As illustrated in this figure, the 3D-Var package can be used not just for (1) general assimilation but as well, and at least, for (2) identification of observation outliers (background check), (3) monitoring (determination of O-P only), (4) testing using single observation experiments, and (5) stand-alone analysis splitting. The term "analysis splitting" that is discussed below in greater detail refers to the process of transferring increments for fields where observations were or are available to correlated model state fields for which observations are not available. This and the optional scaling of error standard deviations shown as part of the figure are two of the various features implemented as part of the 3D-Var-Chem.

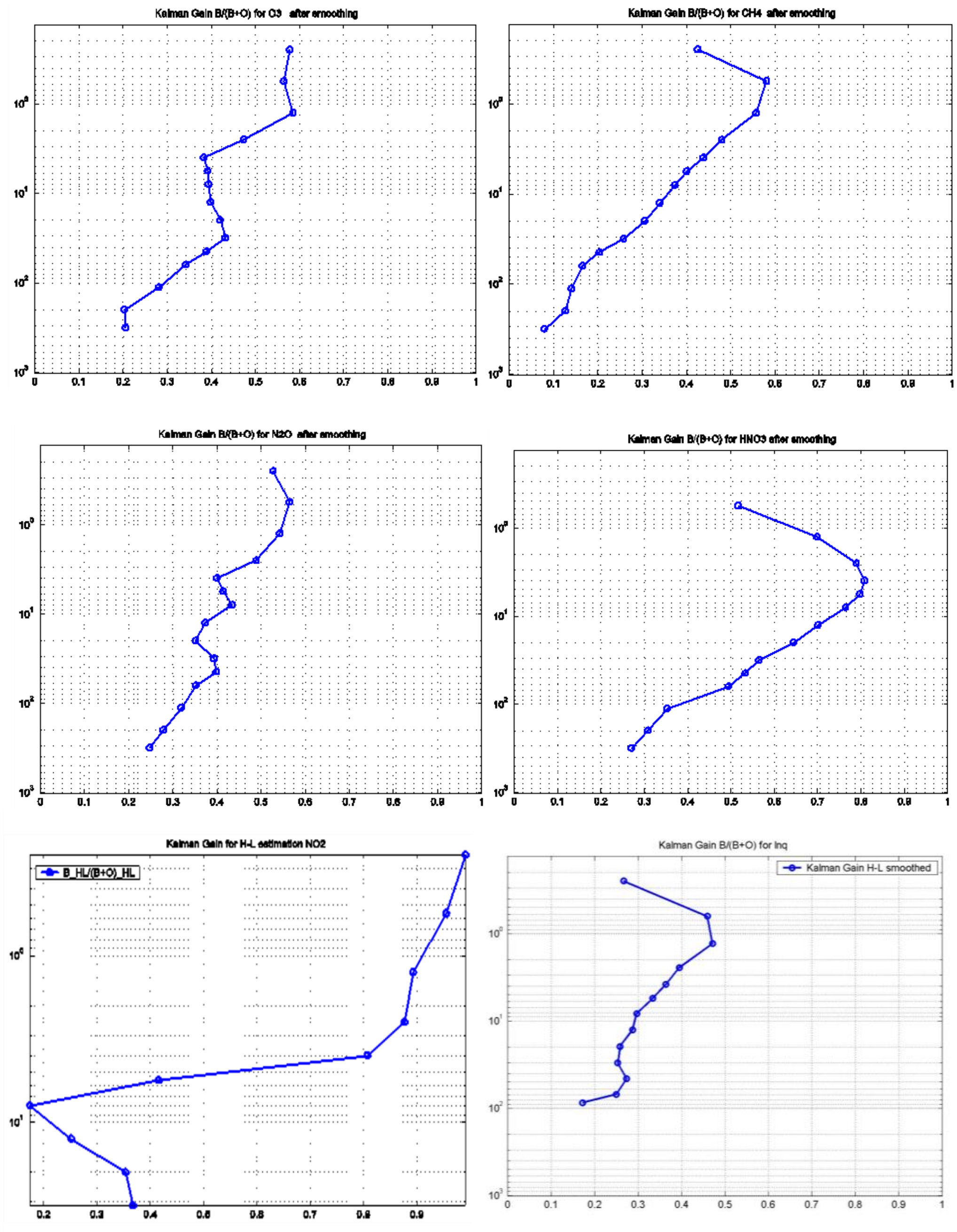

Figure S2. Scalar gain for O_3, CH_4 (from left to right) top row, N_2O, HNO_3 middle row and NO_2 and logarithm of H_2O bottom row.

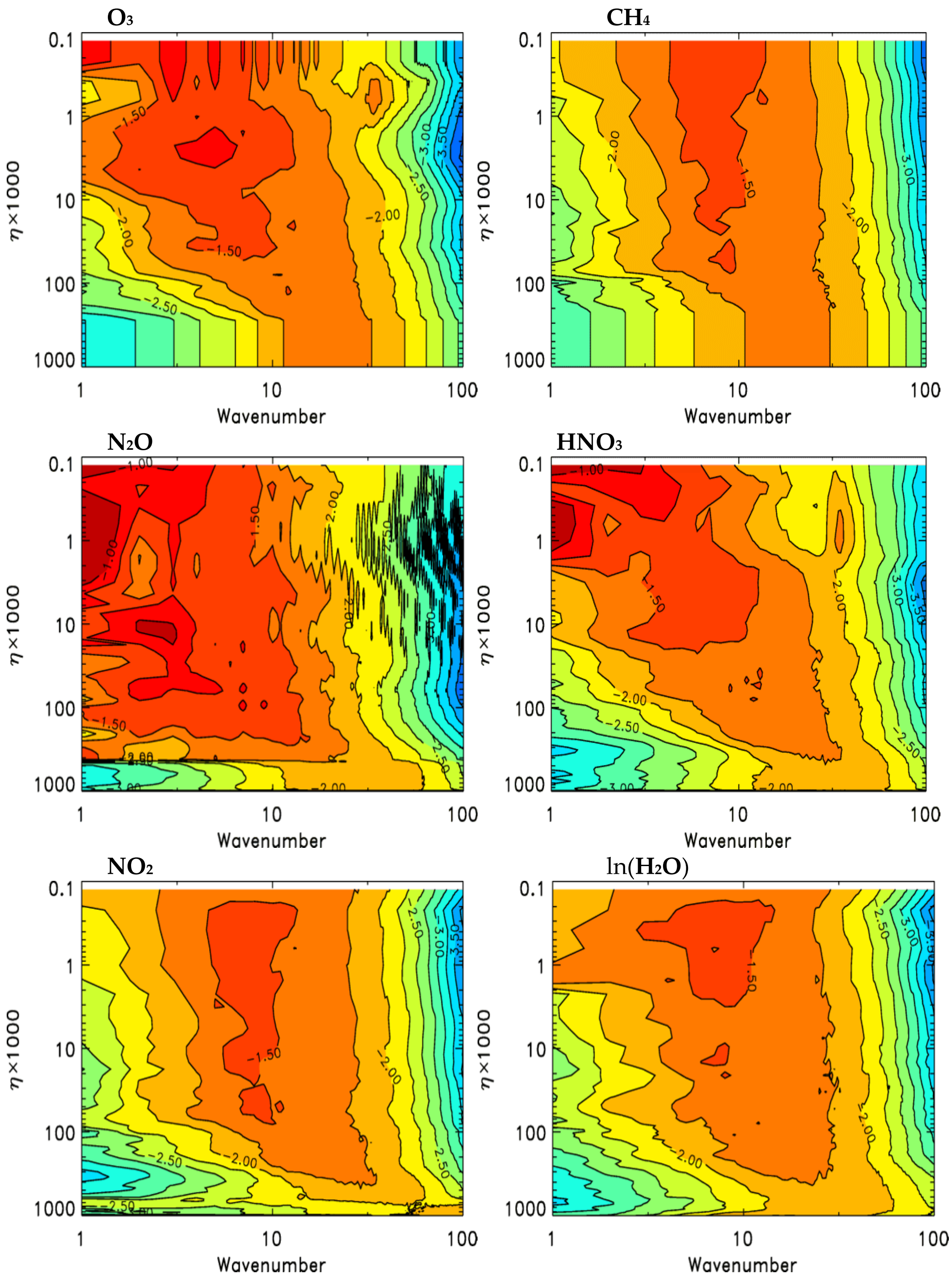

Figure S3. Background error correlation spectra from 6hr-difference method. From left to right, O_3 and CH_4 top row, N_2O and HNO_3 middle row, and NO_2 and $\ln(H_2O)$ lower row.

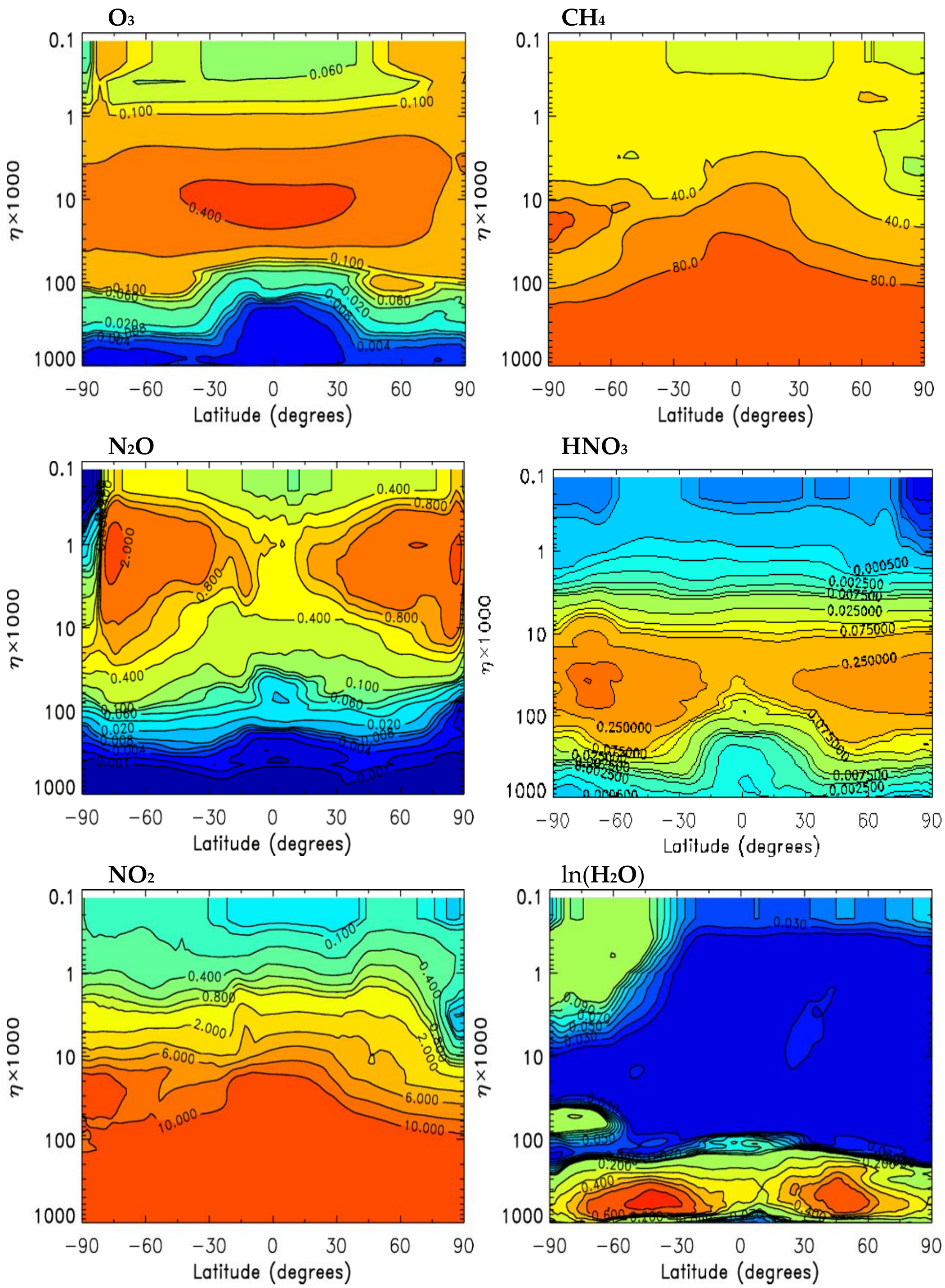

Figure S4. Background error variance from 6hr-difference method. From left to right, O_3 and CH_4 top row, N_2O and HNO_3 middle row, and NO_2 and $\log(H_2O)$ lower row.

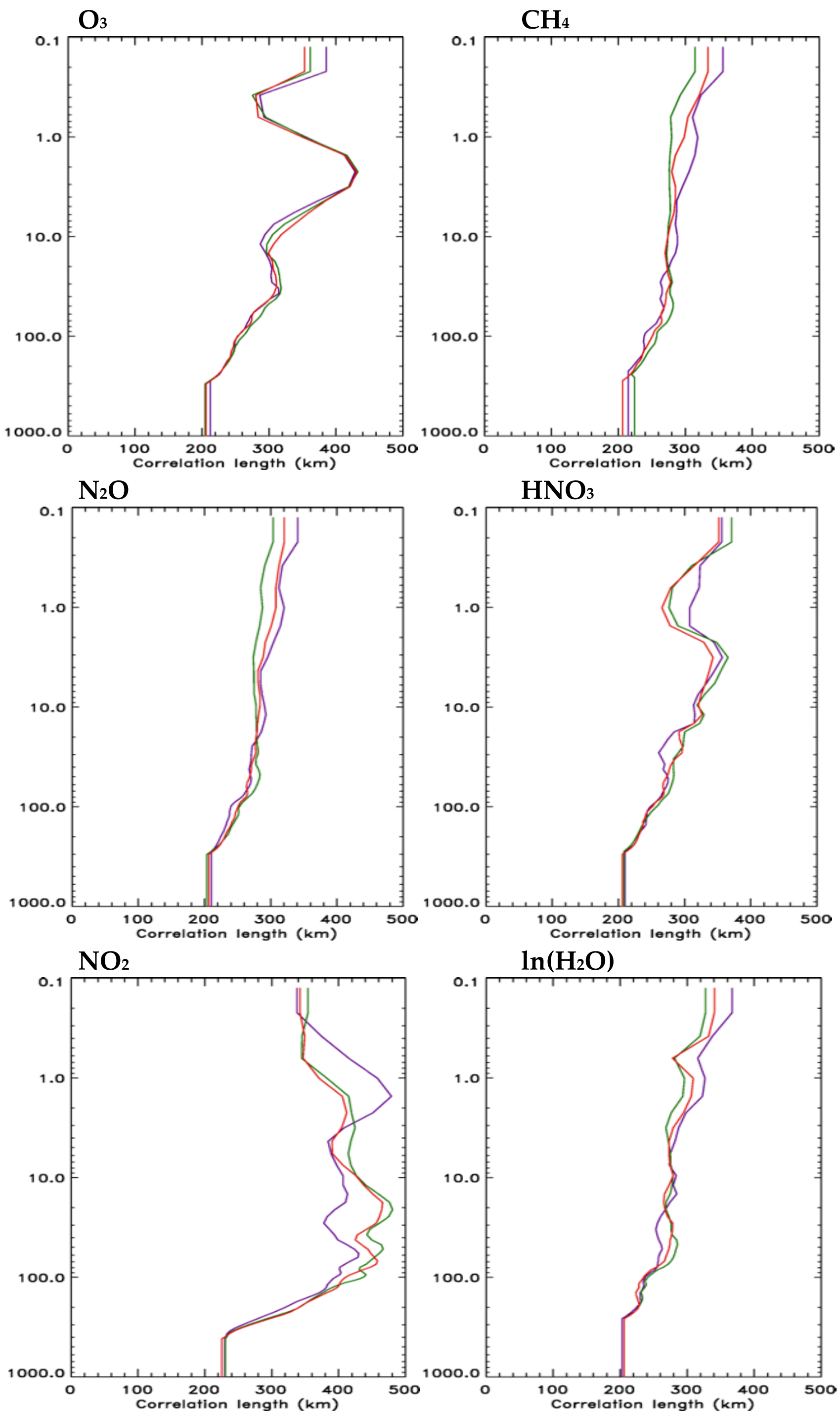

Figure S5. Horizontal correlation length. From left to right: O_3, CH_4 top row, N_2O, HNO_3 middle row, and NO_2 and $ln(H_2O)$ bottom row.

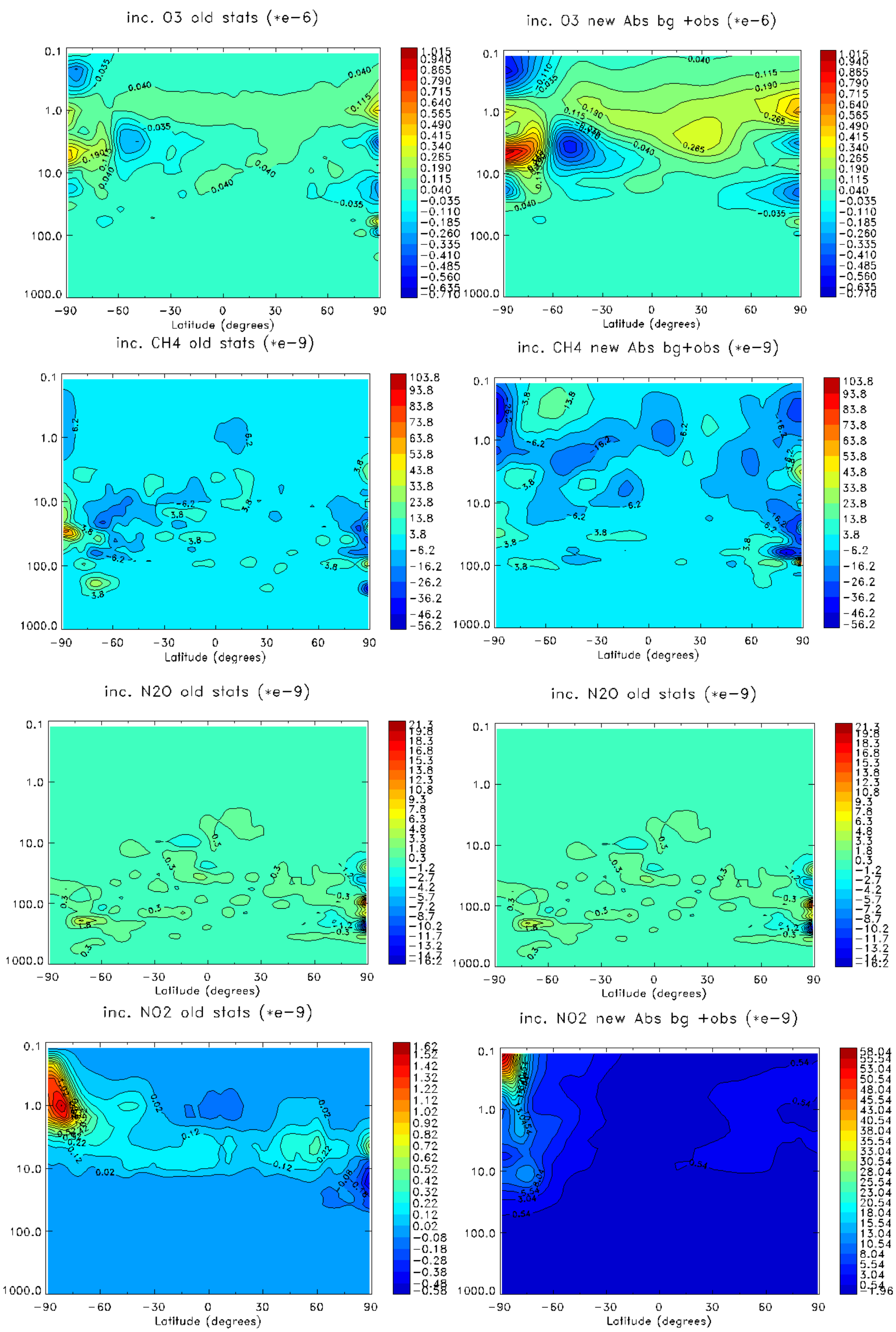

Figure S6. Mean analysis increment for O_3, CH_4, N_2O, NO_2 (from top to bottom) for the period of August 17 to Septemeber 5, 2003. Left panel using the first guess or old error statistics. Right panel using the new error statistics consisting in CQC error correlation and HL error variances.

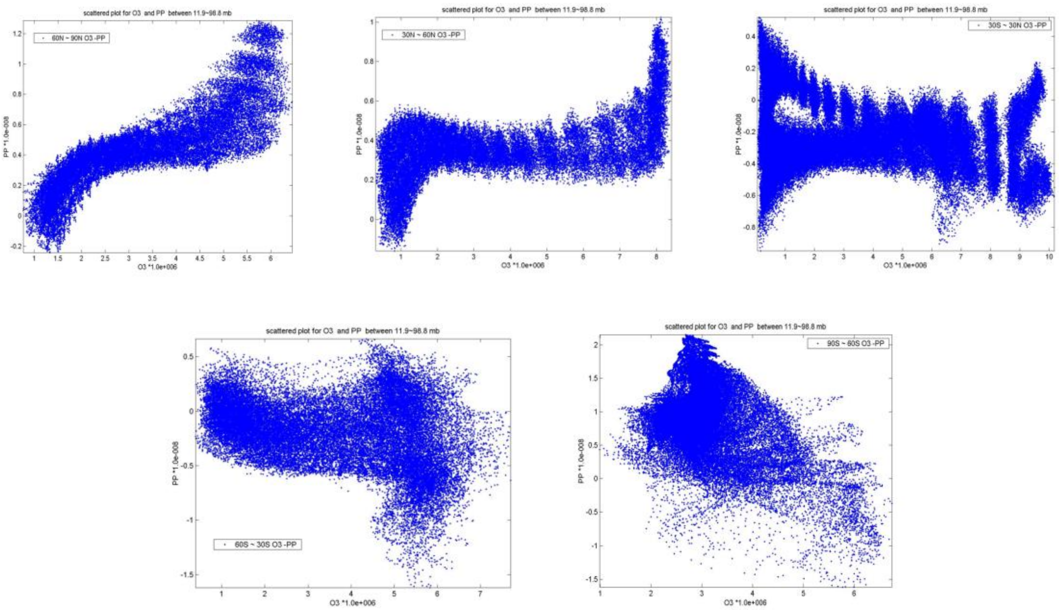

Figure S7. Scatter of O_3 and streamfunction values between 10 and 100 hPa for the month of March 2003.

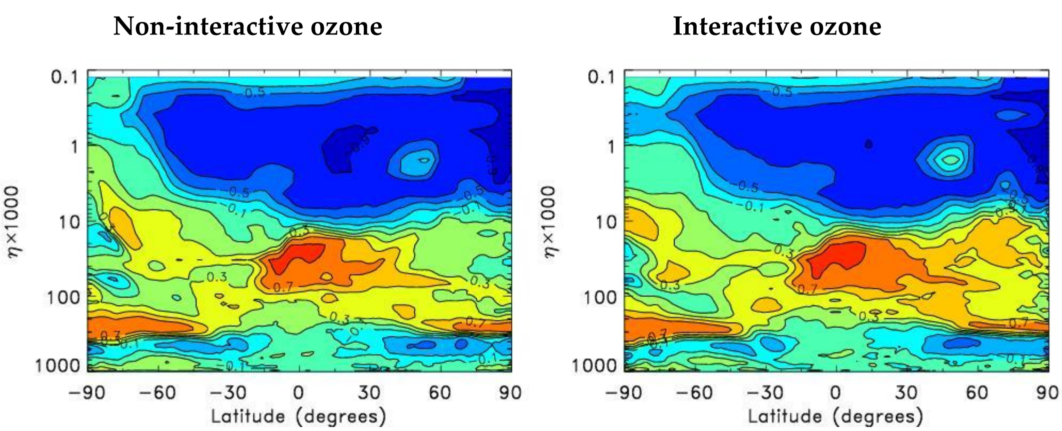

Figure S8. Cross-correlation between ozone and temperature derived from the 24-hr difference (i.e. CQC) method for July 2003. Left panel is for a non-interactive ozone-radiation run of GEM-BACH and right panel for an interactice ozone-radiation run.

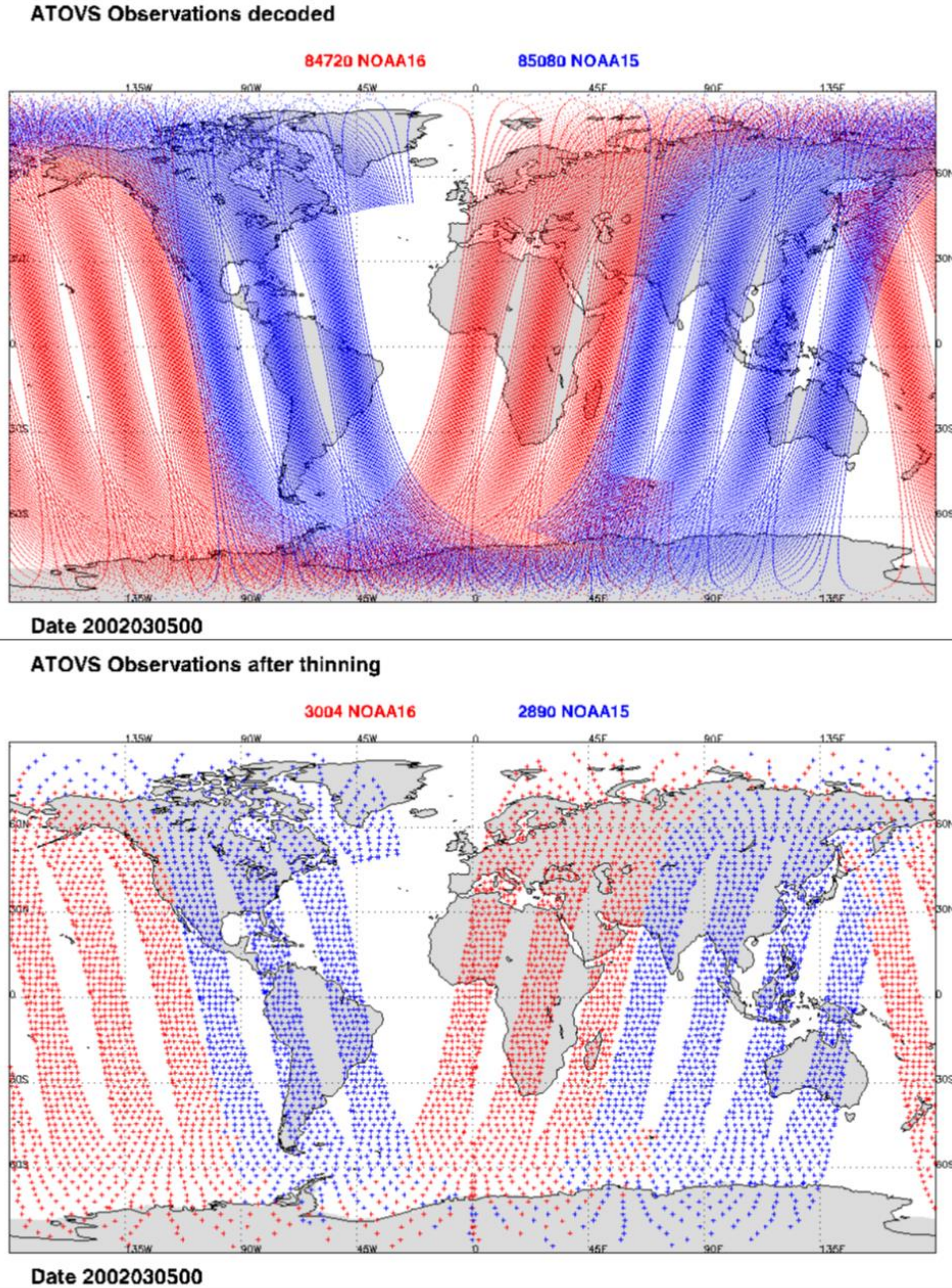

Figure S9. Horizontal coverage of AMSU-A profiles in 6 hours. Upper panel are all profiles, lower panel are the thinned profiles used for data assimilation.

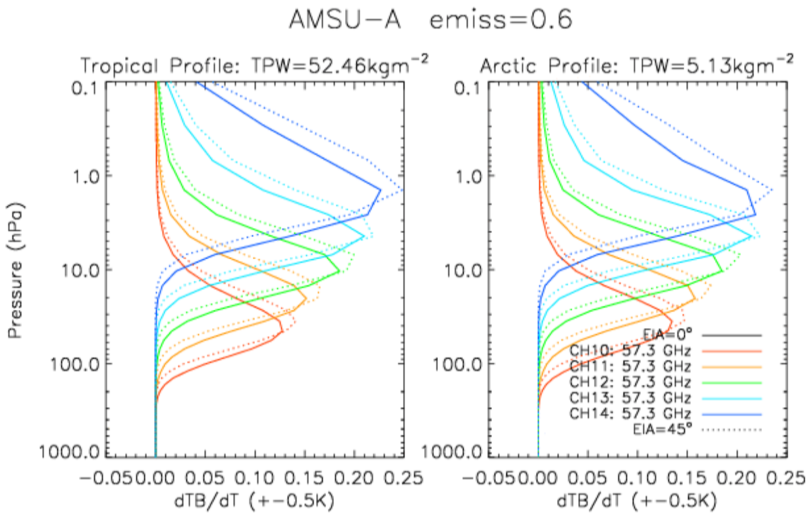

Figure S10. Sensitivity matrix of brightness temperature over temperature for channels 10-14 of AMSU-A. Left are profiles for Tropical air mass, right profiles for Arctice air mass. Solid curves are for nadir measurements and dotted lines

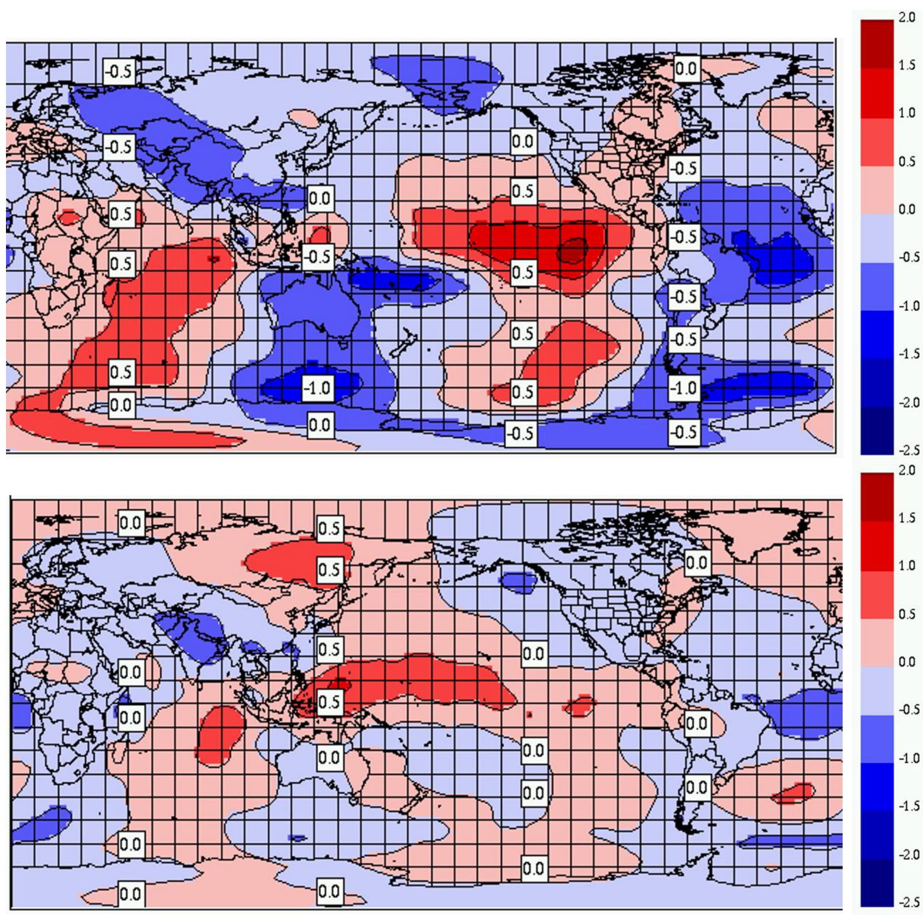

Figure S11. Mean analysis increment at 10 hPa for the month of September 2003. Upper panel using the standard AMSU-A bias correction. Lower panel using the new AMSU-A bias correction based on assimilation of MIPAS temperature only in the stratosphere.

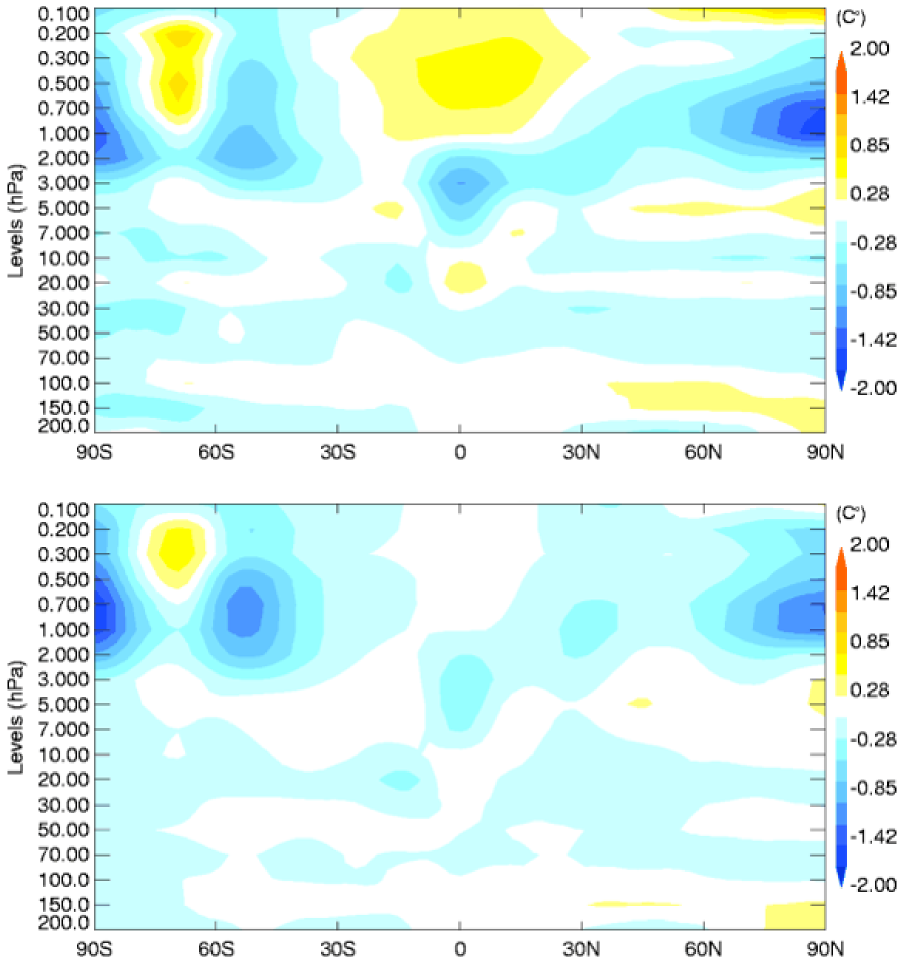

Figure S12. Zonal mean analysis increment for September 2003. Upper panel using the standard AMSU-A bias correction. Lower panel using the new AMSU-A bias correction based on assimilation of MIPAS temperature only in the stratosphere.

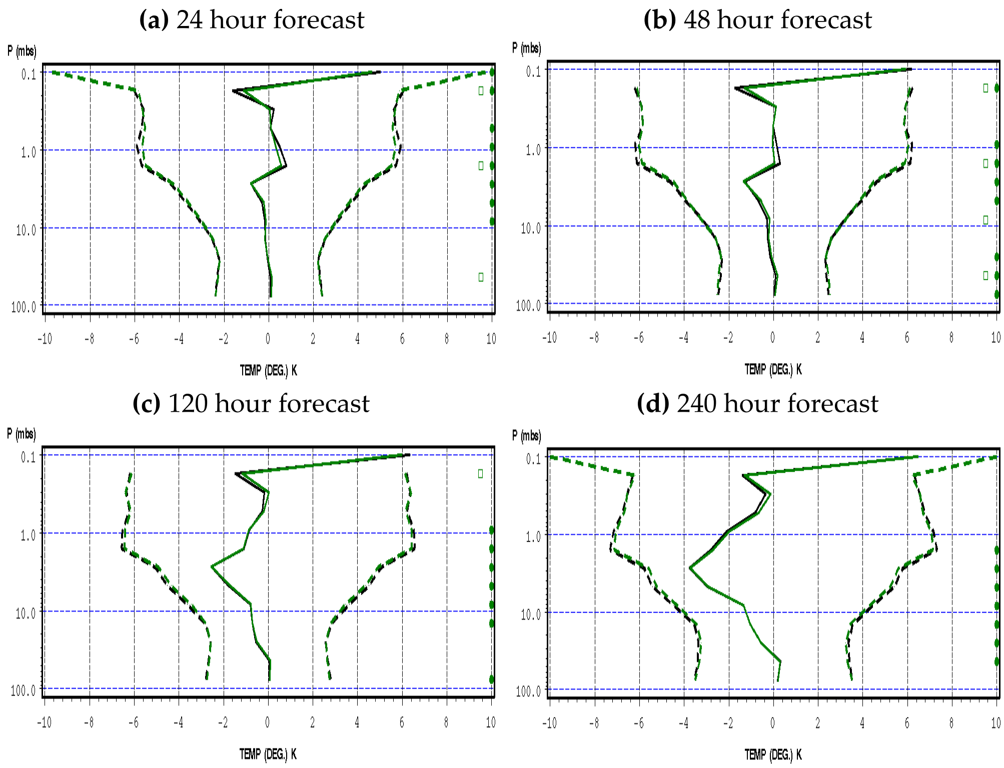

Figure S13. Global verification of observation-minus-forecast temperatures for different forecast lead time. In green, is the assimilation of MIPAS temperatures and AMSU-A with no stratospheric channels, and in black is the assimilation of MIPAS temperatures with all the AMSU-A channels. Verification is made against MIPAS temperatures. Panel (a) is the verification using a one day forecast, panel (b) a two day forecast, panel (c) a five day forecast, and panel (d) a 10 day forecast.

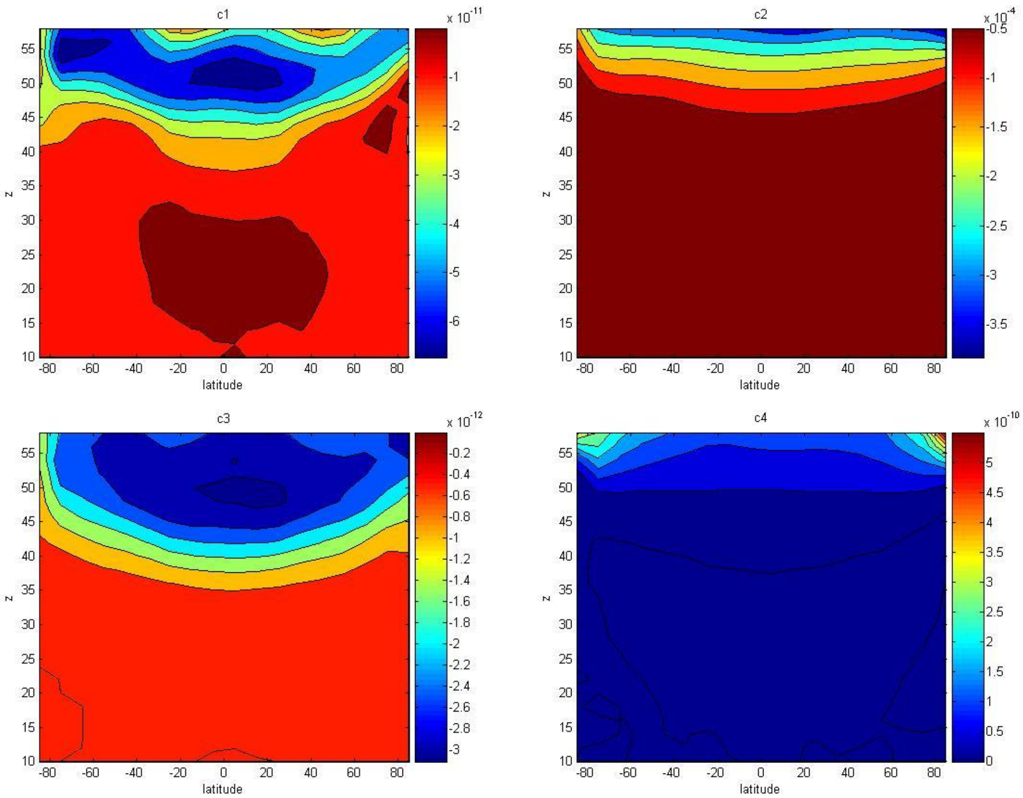

Figure S14. Coefficients of the LINOZ scheme for September. Upper left panel c_1 (10^{-11} volume mixing ratio s^{-1}), upper right panel c_2 (10^{-4} s^{-1}), lower left panel c_3 (10^{-12} volume mixing ratio °K^{-1}), lower right panel c_4 (10^{-10} volume mixing ratio DU^{-1}). The pressure altitudes (km) are $z = 16 \log_{10}(10^5/p)$ where the pressure p is in Pa

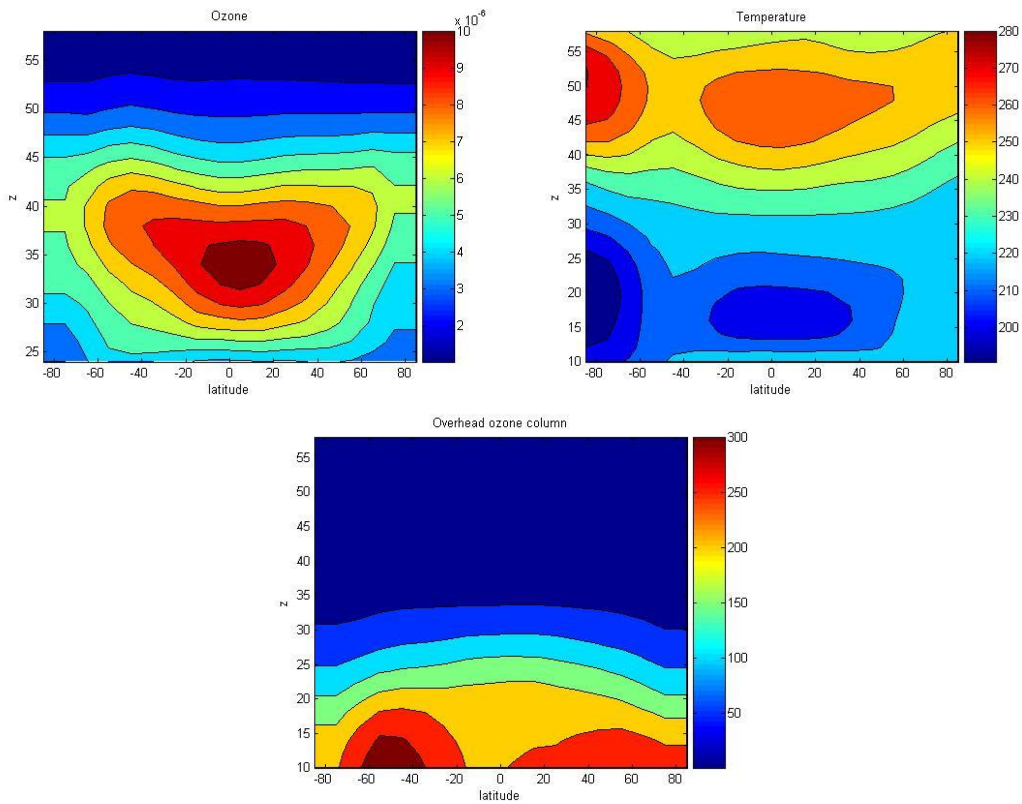

Figure S15. LINOZ climatology for September. Ozone in the upper left panel ozone (10^{-8} volume mixing ratio), temperature in the upper right panel (°K), overhead ozone column in the lower left panel (units DU).

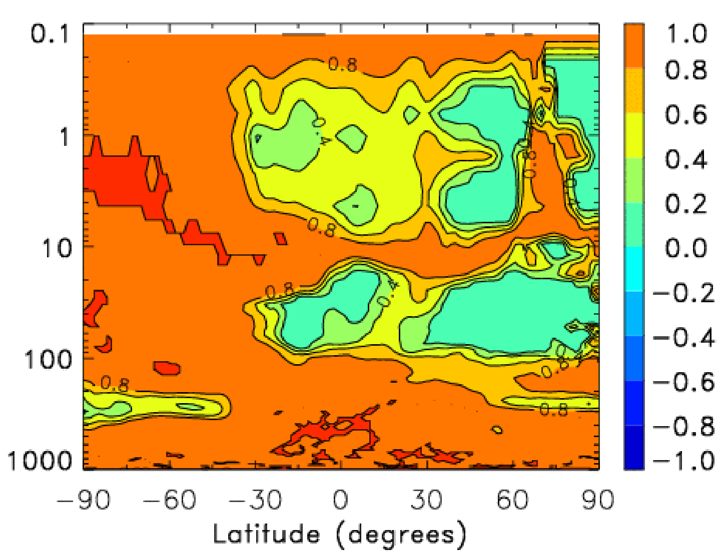

Figure S16. Ratio of unexplained variance to the total variance for the balance operator $\mathbf{A}^{CQC-NMC}$.

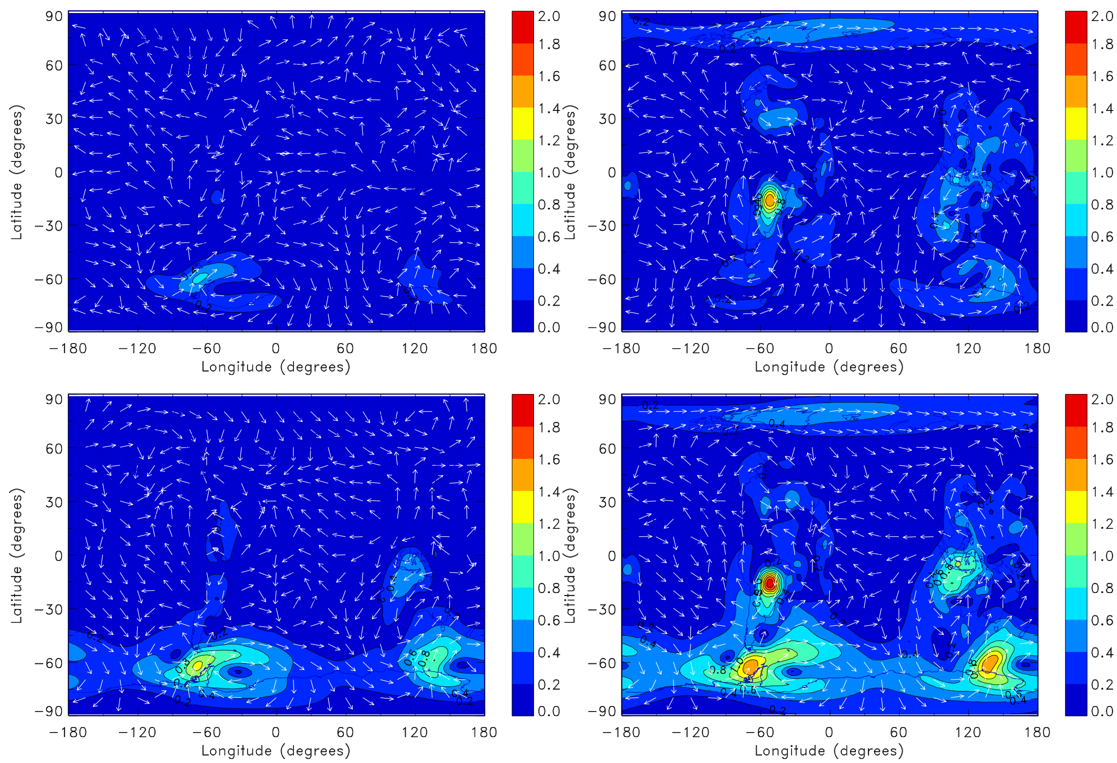

Figure S17. Same as Figure 19 but at 50 hPa

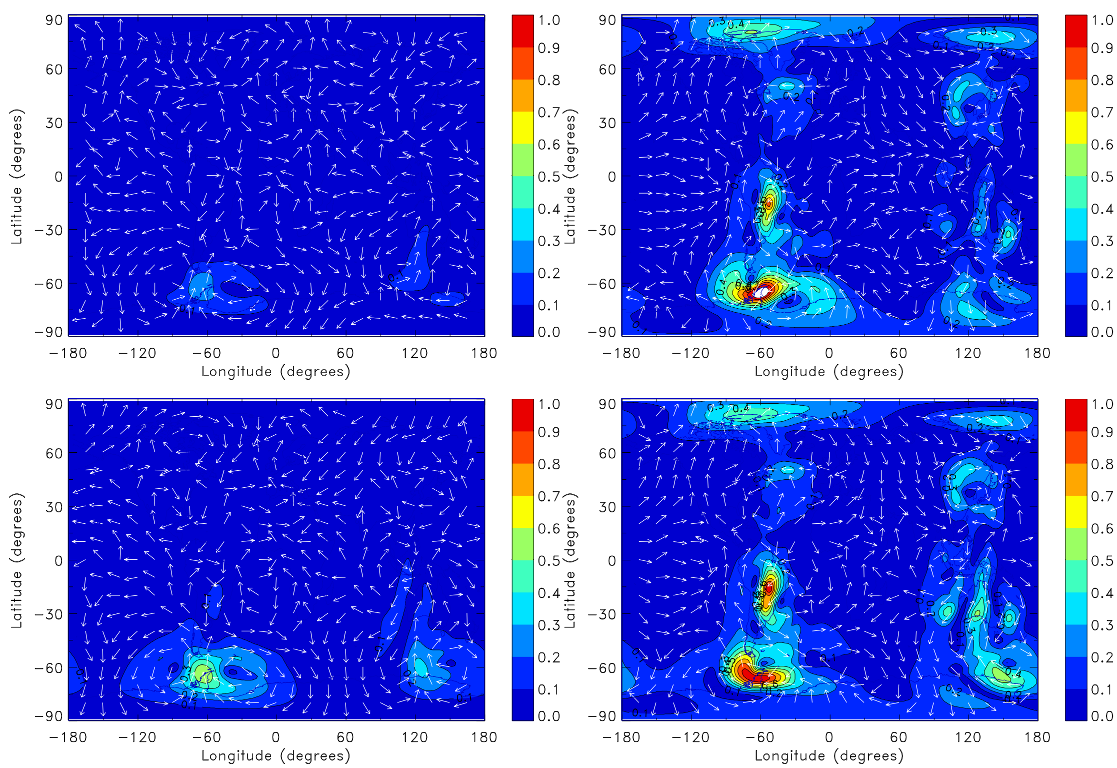

Figure S18. Same as Figure 19 but at 100 hPa

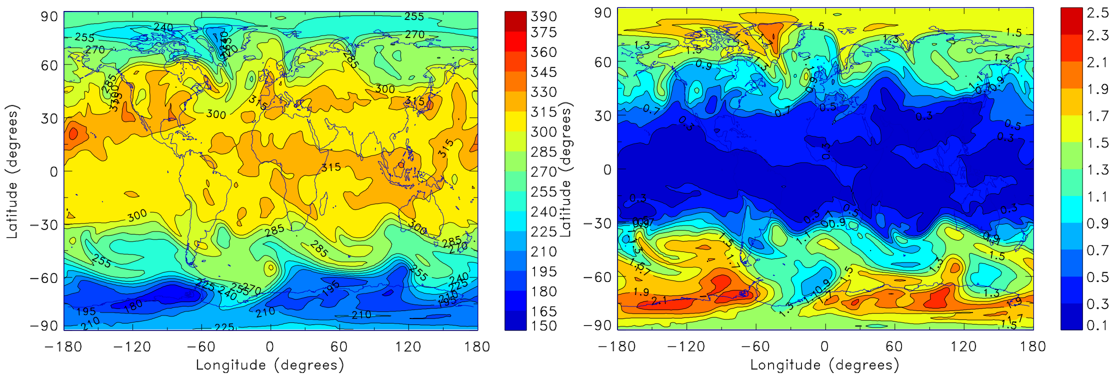

Figure S19. Analysis of N_2O (left panel) and O_3 (right panel) at 100 hPa on August 11, 2003, 00 UTC.

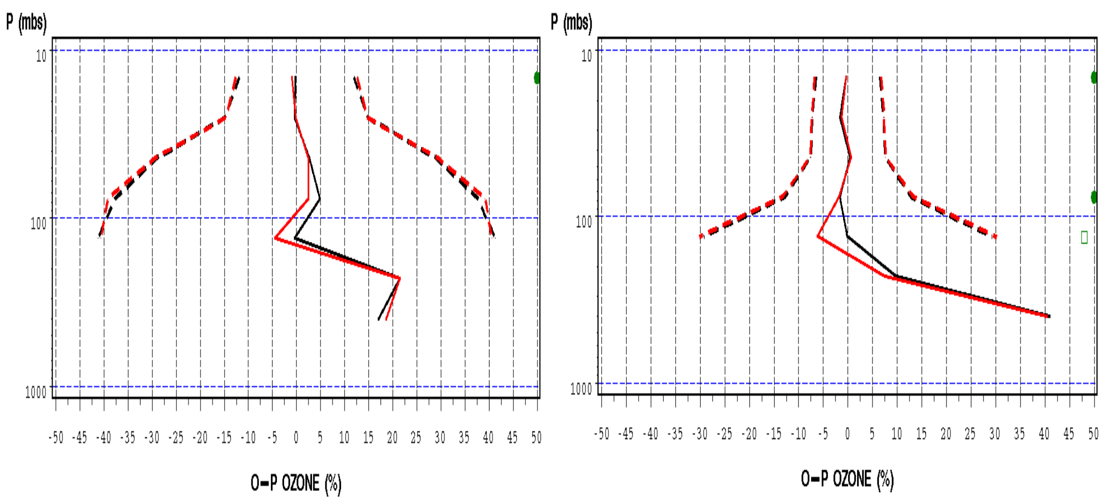

Figure S20. OmP ozone comparison against MIPAS for the 3D-Var assimilation cycle (black) and 4D-Var (red) for the period September 20 to October 5, 2003 over the South Pole region (left) and Southern Hemisphere mid-latitudes (right).